Available online at www.sciencedirect.com

ScienceDirect

Mendeleev Commun., 2019, **29**, 693–695

Mendeleev Communications

Phase diagram of the monoethanolamine–dioxane system

Irina A. Solonina,*[a] Margarita N. Rodnikova,[a] Mikhail R. Kiselev,[b] Andrey V. Khoroshilov[a] and Sergey V. Makaev[a]

[a] *N. S. Kurnakov Institute of General and Inorganic Chemistry, Russian Academy of Sciences, 119991 Moscow, Russian Federation. E-mail: solonina@igic.ras.ru*

[b] *A. N. Frumkin Institute of Physical Chemistry and Electrochemistry, Russian Academy of Sciences, 119991 Moscow, Russian Federation*

DOI: 10.1016/j.mencom.2019.11.031

The monoethanolamine–dioxane system was examined by the DSC performed at various cooling/heating rates in the temperature range from –140 to +25 °C. Rapid cooling revealed that the system undergoes a glass transition at about –120 °C, while in the case of slow cooling, the crystallization of two dioxane phases was observed at +4 and –20 °C. The phase diagram of eutectic type with strong supercooling of the liquid phase was obtained for this system.

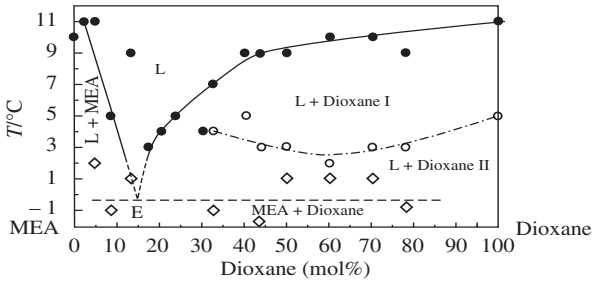

Low-temperature investigations of phase diagrams of solvents containing a spatial network of hydrogen bonds are of practical interest in the cryobiology.[1–4] Monoethanolamine (MEA) is the simplest representative of amino alcohols, the solvents forming the mentioned spatial network of hydrogen bonds, which is characterized by strong supercooling of the liquid phase, a difficult crystal formation, an easy transition to the amorphous state, and total solubility in water. These properties are necessary for cryoprotectors in biological systems at low temperatures, which consequently results in practical applications of aqueous MEA solutions in the cryobiology.[5–8] A presence of the hydroxy group in the MEA molecule and the ability of these molecules to form intramolecular H-bonds significantly reduce the basicity of amino group, which is also important in the cryobiology.[6]

It was of interest whether the freezing point of this solvent could be decreased by the addition of a non-electrolyte to liquid MEA and whether a solvophobic effect exists in its solution. No any solvophobic effect was detected in the MEA–DMSO system in the temperature range of 293–323 K.[9] Dioxane is more solvophobic than DMSO in all of its parameters. The studies performed on the heat capacity and bulk properties of MEA–dioxane liquid system should be also supplemented with data on the solid phase of this system.

Quantum chemistry methods,[10–12] vibrational spectroscopy,[13–15] and X-ray diffraction analysis[16,17] were used to study the conformations of the MEA molecules in gaseous, liquid and solid states. The preferability of *gauche* conformation[10] in the gas phase, the easy conformational transitions in the liquid phase,[18] and the predominance of *trans* conformation in the crystalline state of MEA were reported.[16] MEA is characterized by a large temperature range for its liquid phase with melting point (mp) at 10.3 °C and boiling point (bp) at 170 °C, significant viscosity ($\eta = 18.95 \times 10^{-3}$ Pa s),[19] low self-diffusion coefficient ($D = 0.055 \times 10^{-5}$ cm^2 s^{-1}),[20] low compressibility ($\beta = 38.7 \times 10^{-11}$ Pa^{-1}),[21] and low thermal coefficient of volume expansion ($\chi = 80.7 \times 10^{-5}$ K^{-1}).[21] These values are typical of liquids containing a spatial network of hydrogen bonds.[22]

Dioxane molecule can exist as eight different conformers,[23] while the chair conformation is the most stable form according to the calculated[23] and experimental electron diffraction data.[24] The dipole moment of dioxane molecule is not large (~0.38 D),[25] while the Gutmann donor number (DN_{SbCl_5}) is 14.8.[26] The mp and bp of dioxane are 11.8 and 101 °C, respectively. Dioxane crystallizes in two phases: phase I exists from +11.8 to +5 °C and phase II exists from +5 to at least –140 °C. The molecules are in the *chair* conformation in the both phases.[27]

According to the known data on bulk properties of the H_2O–dioxane system,[28,29] there is a hydrophobic effect in this system, which is manifested due to the presence of a spatial network of hydrogen bonds in water.[22] On the H_2O–dioxane phase diagram,[30,31] they manifest themselves as $C_4H_8O_2 \cdot nH_2O$ clathrate (n = 34–39). Studies of these effects in the liquid phase and their reflection in the solid phase are very important for the area of physical chemistry of solutions.

It was of interest to examine the system formed by dioxane with another solvent that, like water, forms the spatial network of hydrogen bonds in the liquid phase and to compare the MEA–dioxane phase diagram with those of similar systems in order to identify the effect of spatial network of H-bonds of the solvent and the role of non-electrolyte on the nature of phase transitions. Therefore, the solvent used in cryobiology[5–8] with the spatial network of H-bonds, *viz.* monoethanolamine,[22] and dioxane as an amphiphilic non-electrolyte have been considered in the present work.†

† MEA–dioxane solutions were prepared by a gravimetric method under an anhydrous atmosphere (N_2 flow). MEA (99%) and dioxane (99.8%) from ACROS were used without additional purification. The water content determined according to the Fisher method did not exceed 0.05%. The cuvettes were sampled and filled in a dry chamber under N_2 atmosphere. The thermal behavior of samples was investigated by DSC using TA DSC Q100 Instruments and Mettler DSC 30 devices. The phase transition temperatures were recorded in the scanning mode in a stream of Ar (high purity grade) in the temperature range from +25 to –90 °C. Measurement errors were ±1 °C for the temperature and ±2% for the enthalpy change.

The following thermal effects were observed on DSC thermograms: an exothermic peak corresponding to the sample crystallization (heat evolution), an endothermic peak related to the melting of the sample (heat absorption), and lowering of the baseline at low temperatures due to the glass transition/devitrification process in the samples. The phase transition temperatures for the MEA–dioxane system obtained upon cooling and heating of the sample (at the rate of 3 °C min^{-1}) are given in Table 1.

Upon cooling of the MEA–dioxane samples, three exothermic crystallization peaks were observed at the corresponding crystallization temperatures $T_{cr}(1)$, $T_{cr}(2)$, and $T_{cr}(3)$. Upon an increase in the dioxane concentration, the area of exothermic peak $T_{cr}(3)$ was decreased [$T_{cr}(3)$ corresponds to the MEA crystallization], whereas the areas of exothermal peaks $T_{cr}(1)$ and $T_{cr}(2)$ increased [$T_{cr}(1)$ and $T_{cr}(2)$ values are related to the crystallization of dioxane].

Upon cooling of samples with a low dioxane content (up to ~20 mol%), crystallization [$T_{cr}(3)$] was started in the region from –40 to –30 °C and reflected by an exothermic peak with the intense heat generation. The $T_{cr}(3)$ temperature shifts towards more negative temperatures upon increasing in the dioxane concentration (from –27 °C at 2.46 mol% to –47 °C at 70.47 mol%). The phase transition enthalpy at $T_{cr}(3)$ decreases along with increasing in the dioxane concentration from $\Delta H = -196$ J g^{-1} at ~2 mol% to $\Delta H = -35$ J g^{-1} at ~70 mol%.

During cooling of the samples with the dioxane concentration varied from ~20 to ~80 mol%, two exothermic peaks corresponding to the dioxane crystallization were observed. The temperature of their maxima [$T_{cr}(1)$ and $T_{cr}(2)$] shifts towards more positive temperatures upon the increase in the dioxane fraction, while the enthalpy increases from $\Delta H_{1+2} = -30$ J g^{-1} at ~24 mol% to $\Delta H_{1+2} = -130$ J g^{-1} at ~80 mol%.

If the sample was heated (at the rate of 3 °C min^{-1}), the endothermic melting peaks were observed in the region of positive temperatures since dioxane melts at +12 °C and its transition point between I and II crystalline phases is +5 °C[27]. Figure 1 shows the phase diagram for the MEA–dioxane system, which was plotted according to the recorded phase transition temperatures.

Table 1 Phase transition temperatures of the MEA–dioxane system for different dioxane concentrations.[a]

Dioxane (mol%)	$T_{cr}(1)$/°C	$T_{cr}(2)$/°C	$T_{cr}(3)$/°C	T_{eut}/°C	T/°C	mp/°C
0.00			–38			10
2.46			–27			11
5.05			–28	2		11
8.74			–43	–1		5
13.55			–31	1		9
17.63			–34			3
20.61		–30	–30			4
23.94		–26	–29			5
30.65	–13	–19	–32			4
33.04	–12	–16	–49	–1	4	7
40.75	–14	–18	–36		5	9
43.99		–14	–51	–2	3	9
50.28	–8	–12	–41	1	3	9
60.53	–7	–10	–41	1	2	10
70.47	–5	–14	–47	0	3	10
78.38		–15		–1	3	9
100.00	4	–20			5	11

[a] The cooling and heating rates of samples were 3 °C min^{-1}. T_{eut} and T correspond to the temperatures of eutectic composition melting and conformational transition in the dioxane molecule, respectively.

‡ The phase transition temperatures were measured using a Mettler DSC 30 instrument in the scanning mode in a stream of Ar (high purity grade) for the temperature range from –140 to +25 °C. Measurement error was ±3 °C for the temperature and ±4% for the enthalpy change.

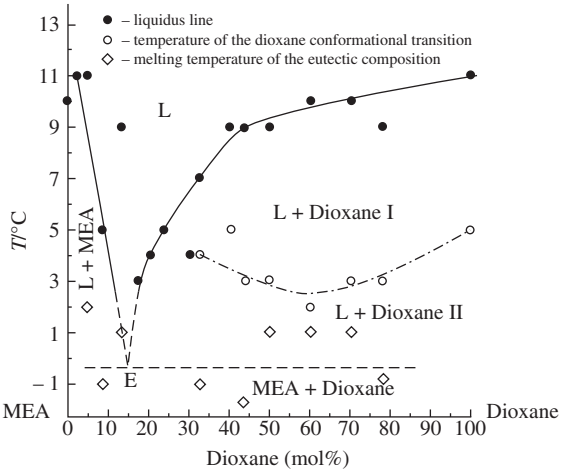

Figure 1 Phase diagram for the MEA–dioxane system recorded at the cooling/heating rates of 3 °C min^{-1}.

When a sample was immersed in liquid nitrogen followed by heating (3 °C min^{-1}), the phase transition temperatures were recorded.‡ These phase transition temperatures for the MEA–dioxane system are given in Table 2.

During the heating, a devitrification effect was observed (baseline drop) on the DSC curve in the low temperature region at T_g of *ca.* –120 °C. Subsequent heating resulted in melting of the eutectic composition and melting of the sample (endothermic peaks). Figure 2 shows the phase diagram of the MEA–dioxane system, which was recorded at fast cooling.

Thus, the liquidus line on the diagram recorded at the cooling rate of 3 °C min^{-1} contains an eutectic at the temperature of ~0 °C and dioxane concentration of ~20 mol%. In the case of fast cooling of the samples, this eutectic shifts towards the high dioxane concentrations (~40 mol%). For slow cooling of the samples it was revealed that MEA–dioxane solutions undergo supercooling, while in the case of fast cooling, these solutions turn into an amorphous state, and the glass transition process occurs.

The possibility to obtain stable (equilibrium) structures in systems based on solvents with a three-dimensional network of hydrogen bonds, such as MEA, arises from a developed spatial network of H-bonds in the solvents themselves and depends on the rate of relaxation processes in them.

Comparison of phase diagrams for systems containing solvents with the spatial network of hydrogen bonds [MEA–dioxane, ethylene glycol(EG)–dioxane, and H_2O–dioxane] revealed that the systems based on MEA and EG with dioxane belong to eutectic

Table 2 Phase transition temperatures[a] of the MEA–dioxane system for different dioxane concentrations.

Dioxane (mol%)	T_g/°C	T_{cr}/°C	T_{eut}/°C	mp/°C
0.00	–127			10
5.05	–121			16
13.55	–120			10
20.61	–120			10
30.65	–119			5
40.75	–117			3
50.28	–121	–48	1	6
60.53	–120	–47	1	4
70.47	–121		1	10
78.38	–119	–82	1	10
100.00				11

[a] The error in temperature measurements was ±3 °C.

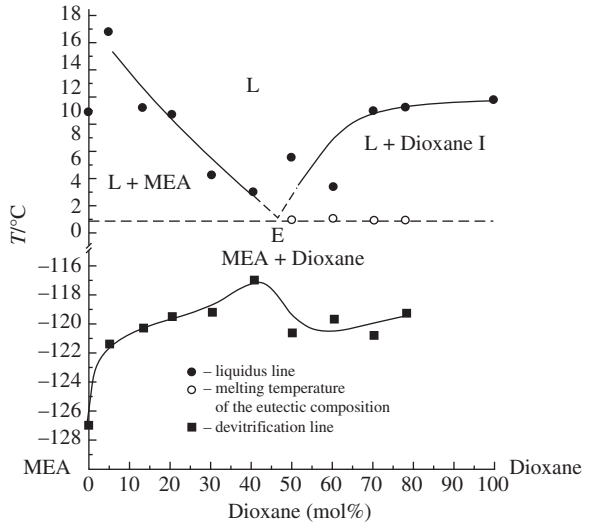

Figure 2 Phase diagram for the MEA–dioxane system recorded at fast sample cooling and heating.

type. In the case of EG–dioxane system, an eutectic was observed at ~16.5 °C and the dioxane concentration of ~10 mol%.[32] The H_2O–dioxane phase diagram,[30] in addition to the eutectic at –15.8 °C and the dioxane concentration of 15.09 mol%, also contains a peritectic at –13.5 °C and the dioxane concentration of 10.7 mol%. The presence of peritectic indicates that the $C_4H_8O_2 \cdot nH_2O$ clathrate exists (n = 36–39).

The absence of a clathrate compound in the EG–dioxane and MEA–dioxane systems can be explained by the smaller lability of the spatial network of hydrogen bonds in EG and MEA as compared to H_2O and a low reactivity of oxygen atoms in the dioxane molecule.

When comparing the phase diagrams for the MEA–dioxane and MEA–tetrahydrofuran (THF) systems, one should pay attention to the structure of non-electrolyte molecules, *viz.* dioxane and THF. The solvophobic components, *i.e.*, four methylene groups in the molecules of cyclic ethers, are different in THF and dioxane. The dioxane molecule contains a second oxygen atom; therefore, it is rigid with a dipole moment of ~0.38 D and a low electron donor capacity (DN_{SbCl_5}) of 14.7. The THF molecule has a dipole moment of 1.74 D and DN_{SbCl_5} = 20. On the MEA–THF phase diagram at medium THF concentrations (from 25 to 60 mol% of THF), the preferred interaction of THF molecules with each other leads to a stratification of the system, which is not observed in the case of MEA–dioxane system.

The differences in the phase diagrams for solvent-based non-electrolyte systems with a spatial network of H-bonds can be explained by the topological features of these spatial networks in H_2O, EG, and MEA and by the difference in the interaction between solvent molecules and molecules of the added non-electrolyte, *i.e.*, dioxane.

In summary, the phase diagram for the MEA–dioxane system was investigated by the DSC method, taking into account not only the temperature and concentration as affecting factors, but also the rates of cooling and heating. The obtained phase diagram belongs to the eutectic type, showing a strong supercooling of the liquid phase from –30 to–40 °C, glass transition at –120 ± 3 °C, the formation of two crystalline phases of dioxane at the crystallization temperatures of +4 and –20 °C, and melting points at +11 and +5 °C, respectively.

This work was supported by the Russian Foundation for Basic Research (grant no. 19-03-00215) and carried out within the framework of the State Assignment (in the field of basic scientific research) to the N. S. Kurnakov Institute of General and Inorganic Chemistry of the Russian Academy of Sciences.

References

1 J. S. Clegg, *Comp. Biochem. Physiol., Part B: Mol. Biol.*, 2001, **128**, 613.
2 E. Shalaev and F. Franks, in *Amorphous Food and Pharmaceutical Systems*, ed. H. Levine, RSC Publishing, Cambridge, UK, 2002, pp. 200–215.
3 M. P. Buera, Y. Roos, H. Levine, L. Slade, H. R. Corti, D. S. Reid, T. Auffret and C. A. Angell, *Pure Appl. Chem.*, 2011, **83**, 1567.
4 L. Slade and H. Levine, *Crit. Rev. Food Sci. Nutr.*, 1991, **30**, 115.
5 P. M. Mehl, *Thermochim. Acta*, 1993, **226**, 325.
6 A. Baudot, C. Cacela, M. L. Duarte and R. Fausto, *Cryobiology*, 2002, **44**, 150.
7 L. Luo, Y. Pang, Q. Chen and G. Li, *CryoLetters*, 2006, **27**, 341.
8 V. I. Grishenko, *Problemy Kriobiologii*, 2005, **15**, 231 (in Russian).
9 I. A. Solonina, D. M. Makarov, G. I. Egorov and M. N. Rodnikova, *Russ. J. Phys. Chem. A*, 2019, **93**, 851 (*Zh. Fiz. Khim.*, 2019, **93**, 685).
10 Yu. V. Novakovskaya and M. N. Rodnikova, *Russ. J. Inorg. Chem.*, 2014, **59**, 1290 (*Zh. Neorg. Khim.*, 2014, **59**, 1534).
11 I. Vorobyov, M. C. Yappert and D. B. DuPré, *J. Phys. Chem. A*, 2002, **106**, 668.
12 C. F. P. Silva, M. L. T. S. Duarte and R. Fausto, *J. Mol. Struct.*, 1999, **482–483**, 591.
13 I. J. Kharitonov, E. G. Khoshabova, M. N. Rodnikova, K. T. Dudnikova and A. B. Razumova, *Dokl. Akad. Nauk SSSR*, 1989, **304**, 917 (in Russian).
14 P. J. Krueger and H. D. Mettee, *Can. J. Chem.*, 1965, **43**, 2970.
15 J. R. Lane, S. D. Schrøder, G. C. Saunders and H. G. Kjaergaard, *J. Phys. Chem. A*, 2016, **120**, 6371.
16 M. N. Rodnikova, I. A. Solonina, A. B. Solovei and T. M. Usacheva, *Russ. J. Inorg. Chem.*, 2013, **58**, 1501 (*Zh. Neorg. Khim.*, 2013, **58**, 1628).
17 D. Mootz, D. Brodalla and M. Wiebcke, *Acta Crystallogr., Sect. C: Cryst. Struct. Commun.*, 1989, **45**, 754.
18 Yu. V. Novakovskaya and M. N. Rodnikova, *Dokl. Phys. Chem.*, 2016, **467**, 60 (*Dokl. Akad. Nauk*, 2016, **467**, 679).
19 A. B. Razumova, *PhD Thesis*, Yaroslavl, 1994 (in Russian).
20 M. N. Rodnikova, F. M. Samigullin, I. A. Solonina and D. A. Sirotkin, *J. Struct. Chem.*, 2014, **55**, 256 (*Zh. Strukt. Khim.*, 2014, **55**, 276).
21 V. N. Kartsev, M. N. Rodnikova, V. V. Tsepulin, K. T. Dudnikova and V. G. Markova, *J. Struct. Chem.*, 1986, **27**, 671 (*Zh. Strukt. Khim.*, 1986, **27**, 187).
22 M. N. Rodnikova, *Russ. J. Phys. Chem. A*, 1993, **67**, 248 (*Zh. Fiz. Khim.*, 1993, **67**, 275).
23 D. M. Chapman and R. E. Hester, *J. Phys. Chem. A*, 1997, **101**, 3382.
24 M. Davis and O. Hassel, *Acta Chem. Scand.*, 1963, **17**, 1181.
25 O. Ya. Osipov, V. I. Minkin and A. D. Granovskii, *Spravochnik po dipol'nym momentam* (*Handbook on Dipole Moments)*, Vysshaya Shkola, Moscow, 1971 (in Russian).
26 A. A. Tager, *Osnovy ucheniya o rastvorakh neelektrolitov* (*Fundamentals of the Theory of Solutions of Non-Electrolytes)*, Izd. Ural. Univ., Ekaterinburg, 1993 (in Russian).
27 J. Buschmann, E. Moller and P. Luger, *Acta Crystallogr., Sect. C: Cryst. Struct. Commun.*, 1986, **42**, 873.
28 R. B. Torres, A. C. M. Marchiore and P. L. O. Volpe, *J. Chem. Thermodyn.*, 2006, **38**. 526.
29 M. Sakurai, *J. Chem. Eng. Data*, 1992, **37**, 492.
30 H. Nakayama and M. Tahara, *Bull. Chem. Soc. Jpn.*, 1973, **46**, 2965.
31 L. Carbonnel and J.-C. Rosso, *J. Solid State Chem.*, 1973, **8**, 304.
32 M. N. Rodnikova, I. A. Solonina, M. R. Kiselev and S. V. Makaev, *Russ. J. Phys. Chem. A*, 2012, **86**, 1745 (*Zh. Fiz. Khim.*, 2012, **86**, 1874).

Received: 13th May 2019; Com. 19/5918